



PII S0016-7037(00)00388-4

Dissolution of albite glass and crystal

JAMES P. HAMILTON,^{1,†} CARLO G. PANTANO,¹ and SUSAN L. BRANTLEY^{2,*}¹Department of Materials Science and Engineering, The Pennsylvania State University, University Park, PA 16802 USA²Department of Geosciences, The Pennsylvania State University, University Park, PA 16802 USA

(Received July 21, 1999; accepted in revised form March 14, 2000)

Abstract—When normalized by initial surface area, crystalline and amorphous albite release Si and Al at the same rate within error ($\pm 40\%$) as measured at pH 2, 5.6, and 8.4 at 25°C. Differences in density and tetrahedral ring structure between the glass and crystal structures, however, lead to more extensive Na and Al depletion from the glass surface, especially in acid. X-ray photoelectron spectroscopy (XPS) indicates that the chemistry of the altered layers on glass and crystal must be significantly different at a depth of $\sim 17\text{Å}$ – 87Å . Nevertheless, angle-resolved XPS (ARXPS) indicates that the outermost 17Å of the glass and crystal surface are compositionally similar. In neutral and weakly basic conditions, XPS indicates less extensive depletion of Na and Al from reacted glass and crystal surfaces than in acidic conditions. Al enrichment was not observed at any pH on either the crystal or glass surface. At steady state, Al release was stoichiometric for all phases and all pH values, but Na release was always faster than release of Si, especially for the glass. These results are consistent with a model where only the outer surface controls dissolution and the deeper layers of the altered surface do not significantly affect dissolution rate. The similarity in dissolution rate between glass and mineral, if consistent for other phases, may also indicate that some future studies of mineral dissolution could be completed more efficiently by investigation of glass because such studies could reveal the chemical effects in dissolution independent of the microstructure and defects that populate natural mineral samples. *Copyright* © 2000 Elsevier Science Ltd

1. INTRODUCTION

Despite extensive investigation of the laboratory dissolution behavior of crystalline feldspar (for a review, see Blum and Stillings, 1995), further studies of feldspar dissolution behavior are necessary for the development of environmental models which can predict groundwater and soil porewater chemistries. Although many dissolution studies have investigated the effects of chemical composition on feldspar dissolution, few studies have investigated the effect of crystallinity on dissolution (Shade, 1981; Tsuzuki et al., 1985; Zellmer and White, 1986; Zellmer, 1986; Yang and Kirkpatrick, 1989; Hellmann et al., 1990b; Hellmann et al., 1991; Hellmann, 1997c). Chemically durable sodium-aluminosilicate glasses (such as albite) may also provide excellent matrices for the immobilization of radioactive fission products (Shade, 1981; Zellmer and White, 1986). A more complete understanding of the dissolution behavior of both glass and crystal of feldspar composition would provide insight for the development of quantitative models of the dissolution reaction, in general.

1.1. Models for Feldspar Dissolution

Three types of models have been developed to describe mechanisms of feldspar dissolution. The first type, now generally discredited, assumes diffusion-controlled kinetics in which the overall feldspar dissolution rate is controlled by the inward diffusion of reactants and the outward diffusion of hydrolysis products through an altered surface layer (for a review, see Brantley and Stillings, 1996; Brantley and Stillings, 1997). The

second type of model assumes surface-reaction controlled kinetics in which hydrolysis reactions break bridging bonds at the solid/solution interface which determine, directly, the rate of feldspar dissolution. This latter model is supported by spectroscopic studies that do not confirm the presence of leached layers more than a few Ångströms thick (e.g. Petrovic et al., 1976; Berner and Holdren, 1979; Holdren and Berner, 1979; Gout et al., 1997). More widely accepted versions of the surface-reaction model are those based on surface complexation. The proton-promoted dissolution (PPD) model for albite, put forth by Blum and Lasaga (1988); Blum and Lasaga (1991); Brady and Walther (1989); Brady and Walther (1992), and Schott (1990) was adapted from the surface protonation model of Stumm and other workers (e.g. Furrer and Stumm, 1986) for simple oxides. Gautier et al. (1994), Oelkers et al. (1994), Oelkers and Schott (1995a,b) developed another surface complexation model that explains control of feldspar dissolution rates by the decomposition of an Al-deficient, silica-rich precursor complex. In these models, the feldspar dissolution rate is proportional to the activity of the (precursor) surface complexes.

A third model combines ideas from both the diffusion-controlled and surface-reaction controlled mechanisms already proposed. Based on calculations of the Na and H diffusion coefficients within the altered layers formed in acidic conditions at 300°C (Hellmann, 1995; Hellmann, 1997b), and the presence of adsorbed species (specifically Cl^- and Ba^{2+}) throughout the altered layer (Hellmann et al., 1989; Hellmann et al., 1990a), Hellmann postulated that the structures of altered layers are more open and porous than the unaltered crystal surface (Hellmann, 1997b). This concept is consistent with the observed hydrolysis of aluminosilicate sites in plagioclase causing opening of the structure and facilitating the release of cations

* Author to whom correspondence should be addressed (brantley@geosc.psu.edu).

† Present address: Johns Manville, Inc., Littleton, CO 80162.

Table 1. Summary of solution and surface analyses of reacted albite by previous investigators.

| pH range of solution | Temp. | Observations | Type of analysis | Reference |
|----------------------|-----------|--|------------------|------------------------|
| 0.5–13.1 | 100–300°C | – max Na depletion in acid (1500 Å) and base (1200 Å); minimal depletion in neutral conditions – Al depletion in acidic and neutral conditions; variable in base – Na depletion depth > Al depletion depth | solution | Hellmann et al., 1995 |
| 1.2–11.3 | 25°C | – thin leached layers (<40 Å) over entire pH range; thickness decreased as pH increased – in acid, Na and Al depletion – in neutral conditions, Na depletion; Al enrichment – in base, considerable Al enrichment | solution | Chou and Wollast, 1984 |
| 0.5–10.0 | 225°C | – Na and Al depletion over entire pH range – layer thickness ranged from 10–900 Å; decreased with increasing pH in acid; increased with pH in base | surface | Hellmann et al., 1989 |
| 2.9 | 5–90°C | – Na and Al depletion at 5 and 50°C; little or no depletion at 90°C – layer thickness ranged from 90–500 Å; thickness decreased with increasing temp. | surface | Chen et al., 2000 |
| 3.5, 5.7 | 25°C | – slightly greater depletion of Na and Al at pH 3.5 than 5.7 – layer thickness = 100–200 Å at pH 3.5; 150–300 Å at pH 5.7 | surface | Muir et al., 1990 |

(Casey and Bunker, 1990). Thus, Hellmann proposed a “leached layer-surface reaction” model in which the dissolution rate of feldspar (albite) is controlled by the rate of detachment of Si at the fluid-solid interface (Hellmann, 1995). However, the rate of surface detachment is also influenced by the presence of leached layers, especially due to reactions (exchange, hydrolysis, condensation) occurring within them, such that the overall dissolution process should be viewed as a 3 D process, and not just a 2 D process. The surface layer in this model, however, does not act as a diffusional barrier to dissolution.

A similar model has also been discussed by Brantley and Stillings (Brantley and Stillings, 1996; Walther, 1997; Brantley and Stillings, 1997) for feldspars in acidic solutions (pH < ~5) that combines surface complexation with diffusion of Al^{3+} , H^+ (or H_3O^+), and M^+ (the charge balancing cations) through an altered surface layer. This model suggests that ion exchange of H^+ or H_3O^+ for K^+ , Na^+ , or Ca^{2+} protonates the Al-O-Si surface site and enhances subsequent hydrolysis of Al-O-Si bonds in the surface. Here, again, the layer is not considered a diffusion barrier.

1.2. Altered Layer Formation

Analyses of effluent solutions and reacted albite surfaces by several investigators have revealed significant discrepancies as to the composition and extent of altered surface layers, especially in neutral and basic conditions (Table 1). The weathering of albite at 25°C in a fluidized bed reactor was studied by Chou and Wollast over a pH range of 1.2 to 11.3 (Chou and Wollast, 1984). Based on solution analysis, the authors reported the presence of thin altered surface layers (<40 Å) of varying composition over the entire pH range. At pH 5.1, an altered surface layer about 25 Å thick developed over 263 h in solution with a composition depleted in Na and enriched in both Al and Si. As pH decreased, the layer thickness increased to about 35 Å at pH 1.2 and the composition of the layer became depleted in both Na and Al and enriched in Si. On the other hand, in alkaline conditions (pH > 6.9), the layer thickness decreased to

about 10–15 Å and the composition was considerably depleted in Si and enriched in Al.

Solution analysis of albite reacted at 100–300°C over a pH range of 0.5–13.1 suggested the formation of leached layers during the initial stages of dissolution due to preferential release of Na and/or Al at nearly all pH and temperature conditions (Hellmann, 1994, 1995). Depletion of Na was greatest in acidic and basic pH conditions, but minimal at neutral pH. Maximum Na depletion depths of approximately 1500 and 1200 Å were reported in acidic and basic conditions, respectively. Depletion of Al was observed in acidic and neutral conditions, but was variable in the basic region. At pH < 10, dissolution was essentially congruent and at pH 10–12, either Al or Si was preferentially released. At very high pH (≥ 12), Al was significantly depleted. The maximum reported Al depletion depth was about 250 Å at basic pH conditions. In general, Na depletion occurred to a much greater depth than Al depletion.

Muir and co-workers (Muir et al., 1990) used XPS and SIMS to measure surface compositions and altered layer thicknesses on albite samples reacted in solutions of pH 3.5 and 5.7 at 25°C. XPS indicated slightly greater depletion of Na and Al from the albite surface reacted at pH 3.5 than pH 5.7. SIMS indicated altered layer thicknesses of 100–200 Å and 150–300 Å on the albite surfaces reacted at pH 3.5 and pH 5.7, respectively. In another study, XPS and ARXPS of albite reacted at pH 2.9 indicated depletion of Na and Al at 5 and 50°C, but little or no depletion at 90°C (Chen et al., 2000). The estimated depth of Na and Al leaching was between 90 and 500 Å (as measured by XPS and SIMS) at both 5 and 50°C, with more extensive leaching occurring at 5°C.

X-ray photoelectron spectroscopy (XPS) of albite reacted at 225°C (Hellmann et al., 1989; Hellmann et al., 1990a) also indicated Na and Al depletion over a pH range of 0.5 to 10. Sputter profiling with XPS indicated leaching depths ranging from 10 to 900 Å that decreased with increasing pH in the acid region and increased with pH in the basic region. Furthermore, angle-resolved XPS (ARXPS) revealed significant depletion of

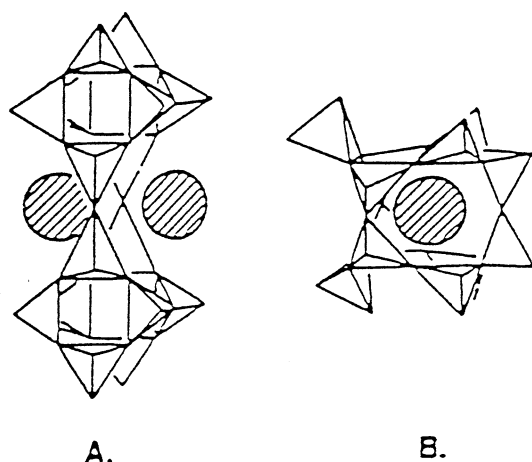


Fig. 1. (A) Schematic of four-membered rings of tetrahedra in crystalline albite with Na ion positions represented by shaded circles. (B) Schematic of six-membered rings in a stuffed-tridymite structure used to describe the structure of albite glass (see text). Figure adapted from Taylor and Brown (1979).

Na and Al from the outer few monolayers of the albite surface. Hydrogen profiles obtained with resonant nuclear reaction analysis (RNRA) indicated a strong pH-dependence of hydrogen incorporation into the albite surface at 300°C (Hellmann et al., 1997a). The greatest penetration occurred in acid, while considerably less penetration was observed in neutral conditions and little or no penetration in base. A similar, pH-dependent trend in the depletion of sodium from the albite surface at 300°C was observed in the RNRA sodium profiles.

The combined surface and solution analyses of these investigators indicates a trend towards altered surface layer formation in acidic conditions, where Na and Al depletion depths range from tens of Å to a few thousand Å. In neutral conditions, a decrease in the layer thickness (tens of Å to a few hundred Å) was generally observed with some variability reported in the composition of the layer; i.e., Na depletion was always observed, but both Al depletion or enrichment (with respect to Si) have been reported. In basic conditions, the reported layer thicknesses and compositions were even more variable. Some authors measured thinner altered layers in basic conditions than in acidic or neutral conditions, while others observed an increase in layer thickness. Again, both Al depletion and enrichment were reported in the basic regime. In conclusion, while it is generally believed that an altered layer forms in acidic conditions, the exact nature of this layer in the neutral and basic regions is still debatable.

1.3. Glass Dissolution Studies

All of the experimental studies discussed thus far have dealt with crystalline feldspars. Only a few studies investigate dissolution kinetics of amorphous albite (Shade, 1981; Tsuzuki et al., 1985; Zellmer and White, 1986; Zellmer, 1986; Yang and Kirkpatrick, 1989; Hellmann et al., 1990b; Hellmann et al., 1991; Hellmann, 1997c). Experimentally measured x-ray radial distribution functions (RDF) (Taylor and Brown, 1979) indicate albite glass is a three-dimensional framework of predom-

Table 2. Comparison of crystalline and amorphous albite dissolution rates.

| Type of experiment | Initial pH | Final pH | Temperature (°C) | Reaction time (hours) | Glass rate/crystal rate |
|--------------------|------------|------------------------------|------------------|-----------------------|-------------------------|
| Flow ^a | 2.0 | 2.0 | 25 | 3638 | 0.8 |
| Flow ^a | 5.6 | 5.6 | 25 | 5416 | 2.2 |
| Flow ^a | 9.3 | 8.4 | 25 | 5416 | 2.5 |
| Batch ^b | 2.0 | 2.3 | 70 | 505 | 1.6 |
| Batch ^b | 3.0 | 4.1 (crystal) 4.3 (glass) | 70 | 505 | 1.6 |
| Batch ^b | 4.0 | 5.6 (crystal) 7.4 (glass) | 70 | 505 | 1.0 |
| Batch ^b | 5.6 | ? | 70 | 505 | 2.5 |
| Batch ^b | 10.0 | 9.7 | 70 | 505 | 2.8 |
| Batch ^c | DI water | ? | 90 | 672 | 1.0 |
| Flow ^d | 3.4 | 3.4 | 300 | 24 | 1.8–3.2 |
| Flow ^d | 5.7–11.0 | 5.7–11.0 | 300 | 24 | 3.2–31.6 |

^a Data from this study.

^b Zellmer, 1986.

^c Shade, 1981.

^d Hellmann et al., 1990b.

inantly six-membered rings of Si- and Al-tetrahedra, while the albite crystal contains mainly four-membered rings of tetrahedra (Fig. 1). Molecular orbital calculations in conjunction with Raman spectroscopy of fully-polymerized aluminosilicate glasses (including the albite composition) have indicated the likelihood of three- and four-membered rings, in addition to six-membered rings, within the glass structure (Kubicki and Sykes, 1993; Sykes and Kubicki, 1996).

The standard Gibbs free energy of formation for albite glass is 41.2 kJ/mole greater than that for crystalline albite at 25°C (Robie et al., 1978). However, Shade (1981) reported similar Si release rates for crystalline and amorphous albite under static conditions in deionized water at 90°C. Zellmer and White's study (Zellmer and White, 1986; Zellmer, 1986) indicated that albite glass releases Si at a similar or slightly faster than albite crystal under static conditions over a pH range of 2–10 at 70°C (Table 2). Hellmann et al. (1990b) reported a classic (Hellmann, 1994) 'U-shaped' dissolution curve (as reported for crystalline albite) for albite glass over a pH range of 2–12 at 300°C with a minimum rate occurring in neutral conditions. Dissolution rates were higher for albite glass than albite crystal over the entire pH range. The smallest difference in rates occurred at pH 3.4 (0.25–0.50 log units), in comparison to large differences (0.5–1.5 log units) at pH 5.7 and pH 11.0 (Table 2).

In general, dissolution of alkali-aluminosilicate glasses are described by a model in which diffusion-controlled release of alkali ions is concurrent with breakdown of the silicate matrix (see White, 1992; Grambow, 1992; Doremus, 1994 for reviews). Smets and Lommen (1982) proposed that Na⁺ ions associated with AlO₄⁻ tetrahedra are leached by an ion exchange process described by Doremus (1975) that involves interdiffusion of hydrogen (or hydronium) ions from the water with alkali ions in the glass. The initial rate (and depth) of ion-exchange is proportional to the square root of time (parabolic kinetics). In the later stages of dissolution, the rate of alkali release decreases to a steady state value where the diffusional flux of alkalis equals the rate of breakdown at the

solid/solution interface, thus leading to a constant, steady state thickness of the leached layer. Release of silica into solution is almost always linear with time (except for a few exceptions in which silica release was between parabolic and linear (Douglas and El-Shamy, 1967)).

As in some of the dissolution models described for crystalline feldspar above, breakdown of the aluminosilicate glass matrix and release of soluble glass constituents is inferred to be controlled by the surface complexes (Grambow, 1992). Grambow describes the desorption of silica tetrahedra as the rate-limiting step in this mechanism. Since hydrolysis of the four bridging Si-O- bonds is a prerequisite to the release of silicic acid from the glass network, the precursor of the activated surface complex has been described as a (-O-Si(OH)₃) surface group. The overall glass dissolution rate is then modeled to be proportional to the concentration of activated surface complexes within a reaction zone at the glass surface. This model for glass dissolution is similar in form to models that describe control of crystalline feldspar dissolution rates by reactions at the surface and within altered surface layers.

1.4. Objectives

In this research, the dissolution of both crystalline and amorphous albite is compared in acidic, neutral, and weakly basic solutions at ambient temperature and pressure. In this manner, the effect of long-range order on dissolution can be studied while maintaining constant composition. Furthermore, investigation of dissolution and altered surface layer formation in neutral and basic pH at 25°C is necessary since most previous experiments with crystalline albite were conducted in acidic conditions, while most groundwaters can range from acidic to basic at low temperatures. X-ray photoelectron spectroscopy (XPS), angle-resolved XPS (ARXPS), secondary ion mass spectrometry (SIMS), Fourier transform infrared reflection spectroscopy (FTIRRS), and gas adsorption based on the Brunauer, Emmett, and Teller (BET) isotherm were combined to study the composition and structure of the glass and mineral surfaces. Inductively coupled plasma atomic emission spectroscopy (ICP-AES) and mass spectrometry (ICP-MS) were used to determine aqueous concentrations for the calculation of dissolution rates.

2. EXPERIMENTAL PROCEDURES

2.1. Sample Preparation

High purity albite crystals from Amelia Courthouse, Virginia (Wards Scientific) were used in this investigation. Clear crystals with a high degree of homogeneity (with respect to mineral phases such as orthoclase and muscovite) were handpicked. Albite glass was prepared by two methods. The first glass specimen was originally prepared by Zellmer (1986) and further treated by Merzbacher (Merzbacher and White, 1988). In order to produce a homogeneous, bubble-free glass suitable for sectioning into plates and subsequent polishing, ground Amelia albite crystals were melted in a platinum crucible at 1300°C, ground and remelted again. Because the melt was too viscous to pour, the final melting was carried out in a platinum-foil mold. In order to eliminate small bubbles in the glass, the sample was treated in a hot isostatic press at 1300°C and 2500 psi (172 bars) (see Merzbacher and White, 1988). Microprobe analysis and refractive-index measurements indicated the production of a homogeneous glass by this method (Merzbacher, 1987). A second batch of albite glass suitable for grinding into a powder was prepared by melting crushed Amelia albite

Table 3. Spectrochemical analyses (based on a lithium metaborate fusion process followed by ICP-AES analysis of the resulting solution) of albite crystal and glass powder (100–200 mesh) and electron microprobe analyses of polished crystal and glass plates.

| | Stoichiometric albite | Amelia albite crystal powder | Amelia albite glass powder | Amelia albite crystal plate | Amelia albite glass plate |
|---------------------------------------|--------------------------|---------------------------------------|-------------------------------------|--------------------------------------|------------------------------------|
| SiO ₂ (wt.%) | 68.8 | 68.0 | 68.6 | 67.4 | 68.2 |
| Al ₂ O ₃ (wt.%) | 19.4 | 19.7 | 20.2 | 19.6 | 19.2 |
| Na ₂ O (wt.%) | 11.8 | 11.5 | 11.6 | 11.4 | 11.0 |
| K ₂ O (wt.%) | 0.00 | 0.19 | 0.23 | 0.10 | 0.14 |
| CaO (wt.%) | 0.00 | 0.18 | 0.17 | 0.33 | 0.40 |
| MgO (wt.%) | 0.00 | 0.03 | 0.03 | 0.02 | 0.00 |
| Total (wt.%) | 100.0 | 99.6 | 100.8 | 98.9 | 98.9 |

crystals in a platinum crucible at 1550°C in air for 15 h and annealing at 700°C overnight. Again, the high viscosity of the melt produced small bubbles in the glass. No attempt was made to remove the bubbles from this batch of glass. After annealing, small pieces of glass were removed by running cold water on the outside of the crucible.

Albite crystals and glass (from the second batch) were dry-crushed to a 74–149 μm grain size (100–200 mesh) in an agate mortar and subsequently cleaned in high-purity acetone. Spectrochemical analyses of powdered specimens (based on a lithium metaborate fusion process followed by ICP-AES analysis of the resulting solution) and electron microprobe analyses (based on the average of 1 analysis of 3 different areas) of polished plates of the albite crystal and glass (Table 3) indicated only minor deviations from stoichiometric albite. Both batches of glass had nearly identical compositions as measured by spectrochemical analysis. Also, powder x-ray diffraction showed no evidence of crystallinity in the albite glass. The only difference between the 2 batches of glass was the second batch (for powder experiments) contained small bubbles.

Crystal and glass plates (from the first batch) approximately 2 cm × 1 cm × 0.2 cm were cut and one face was polished to 0.01 μm and a final 0.05 μm cerium oxide/chrome oxide polishing step. Oil-based diamond sprays were used instead of water-based sprays in order to reduce the effect of chemical leaching during the polishing process. No attempt was made to orient the albite crystals. After polishing, the samples were ultrasonically cleaned in high-purity acetone for 15 min. and adventitious hydrocarbons were removed by a 30 min ultraviolet ozone cleaning (UVOC) process (Vig, 1992). Finally, the samples were etched in 1N NaOH solution at 80°C for 3 min. to remove the damaged/contaminated surface layer due to polishing. The samples were immediately rinsed in deionized water at 80°C following the etch and blown with nitrogen gas. Before exposure to aqueous solutions, the samples were treated by UVOC again for 30 min. This rigorous sample preparation procedure yielded a clean, smooth crystal or glass surface (which is ideal for surface analysis) with a surface composition similar to the bulk composition as measured with XPS (see Table 4).

2.2. Reactors

The polished crystals and glasses were placed in polyfluorotetraethylene (PTFE) baskets and hung vertically from the top of 2 L high density polyethylene (HDPE) containers. These containers were pre-cleaned in hydrochloric acid, nitric acid, and boiling water. Solutions at pH 2, 5.6, and 9 were prepared with ultrapure HCl and deionized water, deionized water only, and LiOH and deionized water, respectively. Batch reactors were completely filled (V = 2.3 L) and sealed with Parafilm. This procedure prevented the pH from drifting more than 0.3 over 5000 h. The crystal and glass specimens were immersed in these solutions for varying durations up to 5000 h. The containers were placed in an oven maintained at 25° ± 1°C without agitation. The sample surface area to solution volume ratio (SA/V) was approximately 5.0 × 10⁻³ cm⁻¹ for each batch experiment.

In a separate experiment, both polished specimens and powders were reacted in stirred Nuclepore (or modified Nuclepore) flow-through cells

Table 4. XPS and ARXPS analyses of unreacted and reacted albite crystal and glass at 25°C.

| Sample type | Reactor | Final pH | Reaction time (hrs) | Na/Si (17 Å) | Na/Si (87 Å) | Al/Si (17 Å) | Al/Si (87 Å) |
|----------------|------------------------|----------|---------------------|------------------------------|--|------------------------------|--|
| Albite | Stoichiometry | — | 0 | 0.33 (H) 0.46 (L) 0.34 | 0.33 (H) 0.44 (L) 0.33 (H) 0.34 (L) 0.33 | 0.33 (H) 0.35 (L) 0.30 | 0.33 (H) 0.36 (L) 0.30 (H) 0.34 (L) 0.30 |
| Crystal plate | Unreacted ^a | — | 0 | — | — | — | — |
| Crystal powder | Unreacted ^b | — | 0 | — | — | — | — |
| Glass plate | Unreacted ^a | — | 0 | — | — | — | — |
| Glass powder | Unreacted ^b | — | 0 | — | — | — | — |
| Crystal plate | Batch | 2.0 | 1000 | 0.02 | 0.07 | 0.03 | 0.08 |
| Crystal plate | Flow | 2.0 | 3638 | 0.20 | 0.25 | 0.21 | 0.25 |
| Crystal powder | Flow | 2.0 | 3638 | — | 0.25 | — | 0.24 |
| Glass plate | Batch | 2.0 | 1000 | 0.00 | 0.01 | 0.01 | 0.03 |
| Glass plate | Flow | 2.0 | 3638 | 0.00 | 0.00 | 0.01 | 0.01 |
| Glass powder | Flow | 2.0 | 3638 | — | 0.00 | — | 0.00 |
| Crystal plate | Flow | 5.6 | 5416 | 0.19 | 0.28 | 0.25 | 0.29 |
| Crystal powder | Flow | 5.6 | 5416 | — | 0.33 | — | 0.31 |
| Glass plate | Flow | 5.6 | 5416 | 0.07 | 0.05 | 0.37 | 0.31 |
| Glass powder | Flow | 5.6 | 5416 | — | 0.05 | — | 0.33 |
| Crystal plate | Batch | 9.0 | 1000 | 0.22 | 0.20 | 0.23 | 0.29 |
| Crystal plate | Flow | 8.4 | 5416 | 0.32 | 0.34 | 0.35 | 0.36 |
| Crystal powder | Flow | 8.4 | 5416 | — | 0.30 | — | 0.35 |
| Glass plate | Batch | 9.0 | 1000 | 0.12 | 0.21 | 0.15 | 0.26 |
| Glass plate | Flow | 8.4 | 5416 | 0.12 | 0.08 | 0.31 | 0.30 |
| Glass powder | Flow | 8.4 | 5416 | — | 0.09 | — | 0.34 |

^a The atomic percent ratios for the unreacted (polished and etched) plates are presented as the highest (H) and lowest (L) values obtained from analysis of 10 polished specimens prepared in the same manner.

^b The atomic percent ratios for the unreacted powders are presented as the highest (H) and lowest (L) values obtained from analysis of 10 powder specimens prepared in the same manner.

(described in Stillings, 1994; Stillings and Brantley, 1995; Chen and Brantley, 1997) fabricated from polycarbonate and Teflon, which were submerged in a water bath maintained at $25^\circ \pm 1^\circ\text{C}$. These cells (~ 75 ml) were pre-cleaned in a 10% nitric acid solution and rinsed with deionized water. Input solutions of pH 2 (HCl + H₂O), pH 5.6 (DI water), and pH 9 (LiOH + H₂O) were pumped through the cells at a rate of ~ 2 ml/h, resulting in an average residence time of 37.5 h. Cells were agitated at a speed of ~ 30 rpm. Nitrogen was bubbled through a 2N NaOH solution, deionized water, and the neutral and basic input solutions to reduce pH drift due to dissolving atmospheric CO₂. Output solutions were constantly collected through a 0.4 μm filter, acidified with analytical grade nitric acid, and subsequently analyzed for Na, Al, and Si with a Leeman Labs PS 3000UV ICP-AES. Some solutions with extremely low Na, Al, and Si concentrations were analyzed with a Finnigan MAT Element, a double-focusing sector field ICP-MS. Non-acidified output solutions were also periodically collected to monitor pH using an Orion Research 611 pH meter with an Orion Ross combination pH electrode with an accuracy of ± 0.01 pH units. Reactions proceeded until near attainment of steady state was achieved. Here we define the attainment of steady state when the Si concentration is constant with time to within $\pm 10\%$.

2.3. Surface Analysis

2.3.1. Surface area analysis

After reaction in either the batch or flow-through reactors, the polished specimens were rinsed in high-purity acetone and blown with nitrogen gas. The powdered specimens were removed from the flow-through cells, filtered through a 0.45 μm filter paper, rinsed with deionized water, ultrasonicated in high-purity acetone, and dried at 50°C overnight. Surface areas of powders were measured before and after dissolution with a standard multipoint BET gas adsorption technique using Kr as the adsorbate gas (Micromeritics ASAP 2000). Due to the low surface area, the measurements were near the lower limit of the technique and were estimated to be accurate to within $\pm 35\%$.

2.3.2. X-ray photoelectron spectroscopy (XPS)

The outermost 90 Å of the crystal and glass surfaces were analyzed with XPS using a Kratos XSAM 800 spectrometer. Non-monochromatic, MgK α x-rays were used with an anode current of 20 mA at an electron acceleration voltage of 14 kV. The pass energy was set at 40 eV and the analyzed area was approximately 2–3 mm in diameter. Survey scans (0–1200 eV) were collected to determine the elemental species present on the glass and crystal surfaces. The compositions of these surfaces were determined from high resolution scans of the Na KLL, C 1s, O 1s, Al 2p, and Si 2p peaks at a step size of 0.1 eV. The collection time for each peak was adjusted to yield a signal/noise ratio of at least 50/1. Sensitivity factors for the Na KLL, O 1s, Si 2p, and Al 2p peaks were obtained by analyzing the fracture surface of a sodium-aluminosilicate glass (having the molecular formula Na₂O-0.8Al₂O₃-2.2SiO₂) created in a vacuum of approximately 10^{-6} torr and assuming the atomic percents of each element on this clean surface matched the bulk composition measured with spectrochemical analysis. The sensitivity factor for the C 1s peak was obtained by analyzing a poly(ethylene terephthalate) (PET) film. The surface compositions were expressed as atomic percent ratios normalized to the Si 2p peak. Therefore, the atomic percent ratios reported in this study represent the preferential loss of a given element with respect to Si.

Glass and crystal specimens were analyzed at two different angles in order to enhance depth resolution within the outer approximately 90 Å of the sample surface. The analysis depth in XPS is a function of the inelastic mean free path of photoelectrons that originate from a given element in the solid and the angle between the analyzer entrance and the sample surface. The depth from which 95% of the signal originates was calculated with the following equation:

$$D = 3\lambda \sin\theta \quad (1)$$

where D is the analysis depth, λ is the inelastic mean free path of a given element, and θ is the angle between the analyzer entrance and a line parallel to the sample surface (i.e., the takeoff angle). The kinetic

energies of photoelectrons associated with the Si 2p, Na KLL, and Al 2p peaks are similar in oxide materials and consequently, the inelastic mean free paths and analysis depths are similar (see Seah and Dench, 1979). The average analysis depth for these three elements is approximately 87 Å at $\theta = 65^\circ$ and 17 Å at $\theta = 10^\circ$ (note: analysis was not performed at $\theta = 90^\circ$ due to geometric considerations in the Kratos XSAM 800 XPS; tilting the sample to $\theta = 65^\circ$ provided higher count rates and only reduced the analysis depth by 9 Å). It should also be pointed out that XPS averages over the entire analysis depth reported here, so that an analysis depth of 87 Å corresponds to the *average* composition over the outermost 87 Å of the surface.

2.3.3. Secondary ion mass spectrometry (SIMS)

^1H , ^{16}O , ^{23}Na , ^{27}Al , and ^{29}Si elemental depth profiles of the crystal and glass surfaces were obtained with dynamic SIMS using a Cameca IMS/3F spectrometer. A 250 nA, 14.5 KeV, $^{18}\text{O}^-$ primary beam was used. A 150 μm diameter spot was rastered over a $250 \times 250 \mu\text{m}$ area. Positive secondary ions were collected over a 10 μm diameter area in the center of the crater. The crystal and glass surfaces were not coated; a gold TEM grid provided sufficient surface charge stabilization. These conditions resulted in a sputtering rate of approximately 150 Å/min as determined by measurement of the depth of the crater with profilometry.

2.3.4. Fourier transform infrared reflectance spectroscopy (FTIRRS)

FTIRRS spectra of unreacted and reacted albite glasses were obtained on a Mattson Research Series spectrometer from 4000 to 400 cm^{-1} with a SiC glow bar source after a 5 minute nitrogen purge. Spectra were obtained with 100 co-added scans at an iris opening of 25% and a DTGS detector velocity of 6.2 kHz at 2 cm^{-1} resolution. The interferograms were transformed using triangular apodization and the data were zero-filled to increase the spectral point density to 0.5 cm^{-1} . Specular reflectance spectra were obtained using a Spectra-tech attachment. The reflectance spectra were ratioed to the background spectrum of a polished aluminum mirror. This ratioed spectra were then transformed into absorbance spectra by means of a Kramers-Krönig transformation.

3. RESULTS

3.1. Dissolution Rates

Dissolution was undetectable in the batch reactors based upon solution analysis as measured with ICP-AES (detection limits are approximately 0.02 ppm for Si, Al, and Na). For the flow reactors, steady state dissolution rates ($\text{moles}/\text{cm}^2/\text{s}$) were calculated from the expression:

$$\text{Rate} = CQ/(A m) \quad (2)$$

where C is the Si concentration in solution (moles/L), Q is the flow rate (L/s), A is the *initial* specific surface area (cm^2/g), and m is the mass (g). Variation in C (%RSD) ranges from 3 to 18% depending on concentration and variation in Q (one standard deviation in measured flow) is $\pm 5\%$. Variability in specific surface area ($\pm 1\sigma$) measured with Kr for these low surface area powders was estimated by repeat measurements as approximately $\pm 35\%$. A conservative estimate of the propagated error in rate was therefore $\pm 40\%$ ($= (0.18^2 + 0.05^2 + 0.35^2)^{1/2}$). The “steady state” dissolution rates reported in this study were derived from regions at the end of each experiment where the Si concentration was constant with time to within $\pm 10\%$. Values for the parameters in this equation for the glass and crystal and the calculated dissolution rates are reported in Table 5. Dissolution rates based on flow experiments were reported with respect to the measured output solution pH. Figure 2

indicates a slightly faster dissolution rate for crystalline albite at pH 2 than albite glass at short reaction times. However, at longer reaction times, the dissolution rates converged until, at steady state, they were identical within error. For both glass and crystal, the ratio of initial to final rates was < 10 . The logarithm of the steady state dissolution rates of crystalline and amorphous albite at pH 2 (based on the average of 5 data points at the longest reaction times) were -14.4 and -14.5 ± 0.2 moles $\text{Si}/\text{cm}^2/\text{s}$, respectively.

At pH 5.6, the initial rate for both crystal and glass decreased by a factor of 100 before steady state was achieved. Figure 3 indicates similar dissolution rates for crystalline and glassy albite at short reaction times and a slightly higher rate for albite glass at longer reaction times. At short reaction times (and for all pH 2 results), solution chemistry was monitored with ICP-AES. At longer reaction times for pH 5.6 and 8.4 (> 2500 h), the concentrations of Na, Al and Si in solution were analyzed with ICP-MS. The logarithm of the steady state dissolution rates of albite crystal and glass at pH 5.6 (based on the last 5 data points) were -16.0 and -15.7 ± 0.2 moles $\text{Si}/\text{cm}^2/\text{s}$, respectively. At pH 8.4, dissolution of albite glass was slightly faster than crystal at all reaction times (Fig. 4). At this pH, the initial rate decreased by a factor of 10 as steady state was approached. The logarithm of the steady state dissolution rates of albite crystal and glass at pH 8.4 (based on the last 5 data points) were -15.7 and -15.3 ± 0.2 moles $\text{Si}/\text{cm}^2/\text{s}$, respectively. These results corroborate published rate data for crystalline albite (Blum and Stillings, 1995), but represent the only published dissolution rates for albite glass at 25°C (Table 2). In addition, the experiments were maintained for longer reaction times than reported previously and closer attainment of steady state was probably achieved.

3.2. Surface Area

The specific surface area of unreacted albite crystal powder was slightly larger than that of unreacted albite glass powder of the same particle size ($0.058 \pm 0.020 \text{ m}^2/\text{g}$ vs. $0.040 \pm 0.014 \text{ m}^2/\text{g}$ (Table 5)), in agreement with measurements by Zellmer and White (1986) on unreacted albite crystal ($0.051 \text{ m}^2/\text{g}$) and glass ($0.037 \text{ m}^2/\text{g}$) powders (100–200 mesh). After reaction in flowing pH 2 solution, the surface areas of the crystal and glass increased by a factor of 2 and 30, respectively. After reaction in flow reactors at pH 5.6, the surface areas of the crystal and glass increased by a factor of 1.3 and 1.4, respectively. Finally, after reaction in flowing pH 8.4 solution, the surface areas of the crystal and glass increased by a factor of 1.1 and 1.4, respectively (Table 5).

3.3. Surface Analysis

3.3.1. XPS

The surface compositions of the unreacted crystal and glass plates (polished and etched) as measured with XPS and ARXPS are listed in Table 4 as well as XPS of the unreacted powder specimens. ARXPS cannot be performed on powdered specimens and consequently, compositional information is limited to the outer 87 Å of their surfaces. Surface compositions of the unreacted surfaces are presented as the highest and lowest Na/Si and Al/Si atomic percent ratios measured on 10 polished

Table 5. Experimental conditions and dissolution rates for flow-through cells.

| Sample type | Inlet pH | Outlet pH | Average flow rate (ml/hr) | Starting mass (g) | Average [Si] at steady state (ppm) | Average [Al] at steady state (ppm) | Average [Na] at steady state (ppm) | Specific surface area ^c (m ² /g) | Reacted SSA/unreacted SSA | Log dissolution rate ^d (moles Si/cm ² /s) | Na rate/Si rate at steady state | Al rate/Si rate at steady state |
|---|----------|------------------|---------------------------|-------------------|------------------------------------|------------------------------------|------------------------------------|--|---------------------------|---|---------------------------------|---------------------------------|
| Unreacted albite crystal (100–200 mesh) | | | | | | | | 0.058 ± 0.020 | | | | |
| Unreacted albite glass (100–200 mesh) | | | | | | | | 0.040 ± 0.014 | | | | |
| Albite crystal | 2.0 | 2.0 | 2.0 ± 0.1 | 4.005 | 0.42 ± 0.02 ^a | 0.15 ± 0.01 ^a | 0.24 ± 0.07 ^a | 0.117 ± 0.041 | 2.02 | -14.4 ± 0.2 | 0.71 ± 0.40 | 0.37 ± 0.21 |
| Albite glass | 2.0 | 2.0 | 1.9 ± 0.1 | 4.005 | 0.26 ± 0.01 ^a | 0.17 ± 0.01 ^a | 0.33 ± 0.09 ^a | 1.192 ± 0.417 | 29.8 | -14.5 ± 0.2 | 1.56 ± 0.88 | 0.67 ± 0.38 |
| Albite crystal | 5.6 | 5.6 | 2.0 ± 0.1 | 4.008 | 0.012 ± 0.002 ^b | 0.007 ± 0.002 ^b | 0.011 ± 0.002 ^b | 0.074 ± 0.026 | 1.28 | -16.0 ± 0.2 | 1.12 ± 0.63 | 0.60 ± 0.34 |
| Albite glass | 5.6 | 5.6 | 2.0 ± 0.1 | 4.007 | 0.016 ± 0.003 ^b | 0.007 ± 0.002 ^b | 0.046 ± 0.005 ^b | 0.056 ± 0.020 | 1.40 | -15.7 ± 0.2 | 3.45 ± 1.95 | 0.44 ± 0.25 |
| Albite crystal | 9.3 | 8.4 ^e | 1.9 ± 0.1 | 4.010 | 0.025 ± 0.004 ^b | 0.008 ± 0.003 ^b | 0.016 ± 0.002 ^b | 0.063 ± 0.022 | 1.09 | -15.7 ± 0.2 | 0.79 ± 0.45 | 0.32 ± 0.18 |
| Albite glass | 9.3 | 8.4 ^e | 2.2 ± 0.1 | 4.005 | 0.037 ± 0.004 ^b | 0.009 ± 0.002 ^b | 0.092 ± 0.008 ^b | 0.058 ± 0.020 | 1.45 | -15.3 ± 0.2 | 3.03 ± 1.72 | 0.26 ± 0.15 |

^a Based on average of 5 data points as measured with ICP-AES. Reported errors are % RSD.

^b Based on average of 5 data points as measured with ICP-MS. Reported errors are % RSD.

^c Measured with BET using Kr gas as the adsorbing species.

^d Dissolution rate normalized using initial specific surface areas.

^e pH decreased due to CO₂ gas dissolved into solution.

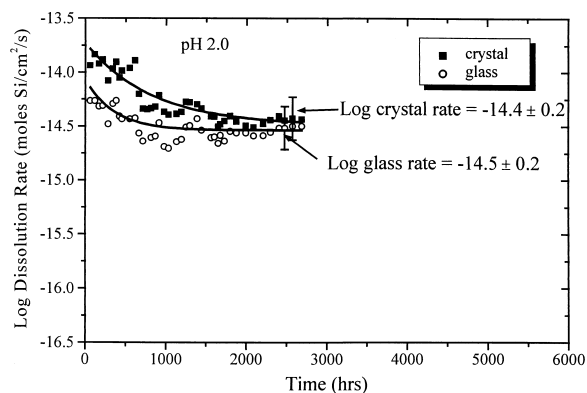


Fig. 2. Log dissolution rate as a function of reaction time in flow experiments (output pH = 2) at 25°C. The dissolution rates for albite crystal and glass at long reaction times are steady-state dissolution rates (see text for rate calculation). Rates are normalized using initial surface areas. For clarity, only every fifth data point is shown. The curves are provided to guide the reader's eye.

plates or 10 powders prepared in an identical manner. Ten analyses of 1 sample of crystal powder and 1 sample of glass powder prepared in an identical manner were performed to test analytical reproducibility. This variability in surface composition due to instrumental error was very small ($\pm 4\%$). Inter-sample variability in the crystal surface composition was probably due to sample heterogeneity and polishing effects, while variability in the glass surface was probably due to polishing effects only. Surface compositions of the crystals and glasses (both polished plates and powders) reacted for long times in batch and flow reactors are also presented in Table 4 as Na/Si and Al/Si atomic percent ratios.

Figures 5–8 present XPS and ARXPS analyses as Na/Si or Al/Si atomic percent ratios vs. reaction time. The highest and lowest Na/Si and Al/Si ratios measured on the unreacted plates are represented as horizontal dashed lines on these plots. Surface compositions of the powder specimens, which were similar to plate specimens (Table 4), are not included in the figures.

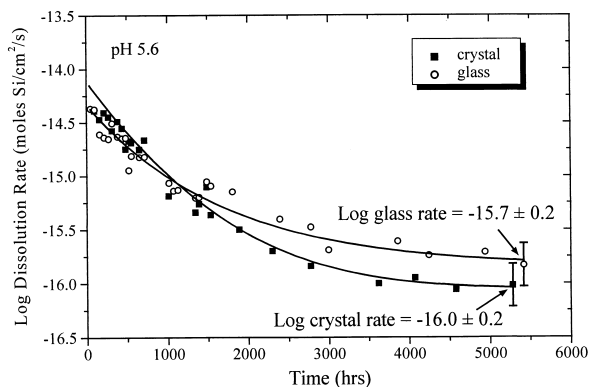


Fig. 3. Log dissolution rate as a function of reaction time in flow experiments (output pH = 5.6) at 25°C. The dissolution rates for albite crystal and glass at long reaction times are steady-state dissolution rates (see text for rate calculation). Rates are normalized using initial surface areas. For clarity, only every fifth data point is shown. The curves are provided to guide the reader's eye.

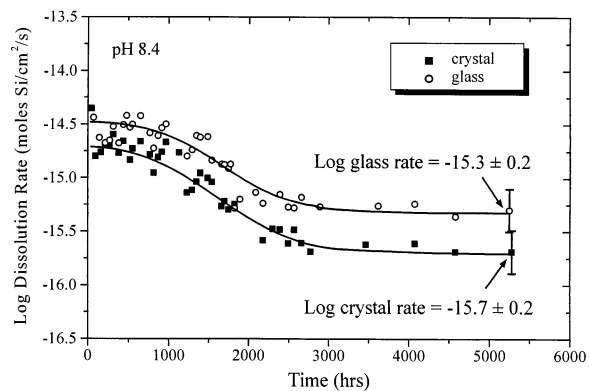


Fig. 4. Log dissolution rate as a function of reaction time in flow experiments (output pH = 8.4) at 25°C. The dissolution rates for albite crystal and glass at long reaction times are steady-state dissolution rates (see text for rate calculation). Rates are normalized using initial surface areas. For clarity, only every fifth data point is shown. The curves are provided to guide the reader's eye.

The XPS and ARXPS results can be summarized in the following statements. Both crystal and glass surfaces (plates and powders) exhibited Na and Al depletion at pH 2. Furthermore,

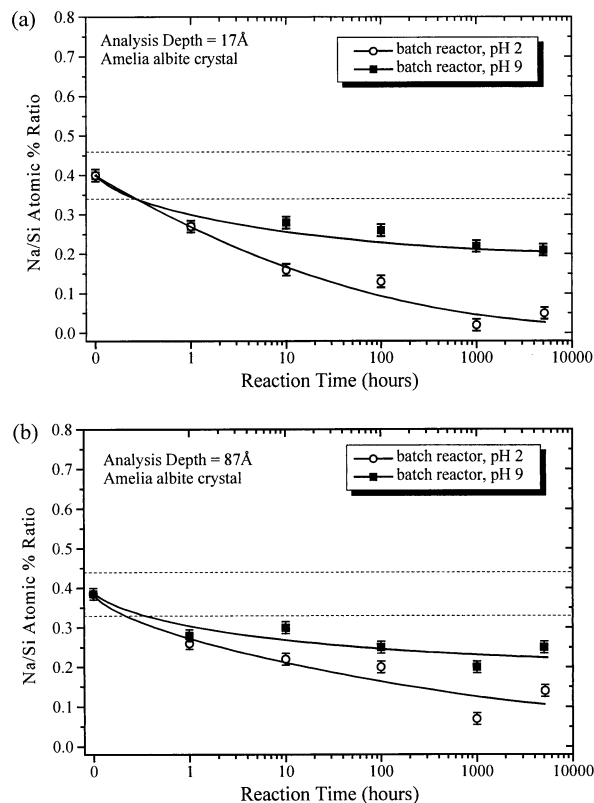


Fig. 5. Na/Si ratios (atomic %) as measured with (a) ARXPS (analysis depth = 17 Å) and (b) XPS (analysis depth = 87 Å), plotted as a function of reaction time for Amelia albite crystal plates in pH 2 and pH 9 solutions in batch reactors at 25°C. The dashed lines represent the highest and lowest Na/Si ratios measured on 10 unreacted, polished crystal surfaces. The curves are provided to guide the reader's eye.

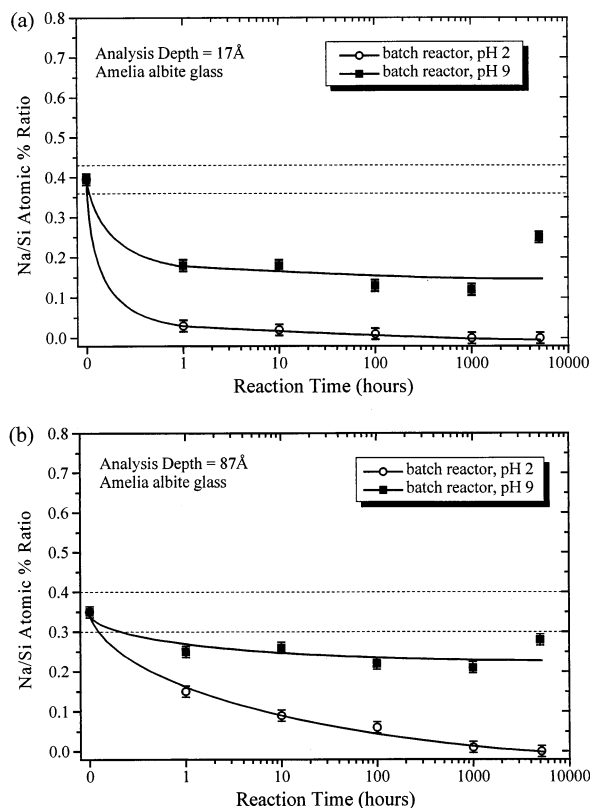


Fig. 6. Na/Si ratios (atomic %) as measured with (a) ARXPS (analysis depth = 17 Å) and (b) XPS (analysis depth = 87 Å), plotted as a function of reaction time for Amelia albite glass plates in pH 2 and pH 9 solutions in batch reactors at 25°C. The dashed lines represent the highest and lowest Na/Si ratios measured on 10 unreacted, polished glass surfaces. The curves are provided to guide the reader's eye.

Na and Al depletion was more extensive in the glass surface than in the crystal surface. As pH increased, the extent of Na and Al depletion from both the glass and crystal surfaces decreased (as exhibited by higher Na/Si and Al/Si ratios). In neutral conditions, the glass surface exhibited more extensive Na depletion than the crystal surface and both surfaces were slightly depleted in Al. In weakly basic conditions, the glass again exhibited more Na and Al depletion than its crystalline counterpart. In general, the glass and crystal surface compositions were more similar within the outer 17 Å than the outer 87 Å. The specimens reacted in batch reactors generally exhibited more Na and Al depletion than specimens reacted in flow cells (Table 4). Finally, no evidence of Li or Cl in the outer 17 Å or 87 Å of the glass or crystal surface was observed with XPS.

3.3.2. SIMS and FTIRs

The sodium, aluminum, and silicon SIMS depth profiles of the reacted crystal and glass surfaces (not presented) were identical to the profiles of the unreacted crystal and glass surfaces. Since the depth sensitivity of SIMS profiling under the experimental conditions was limited to ≈ 200 – 500 Å, surface alteration must have extended ≤ 200 – 500 Å into the surface. This is consistent with XPS that showed gradients in

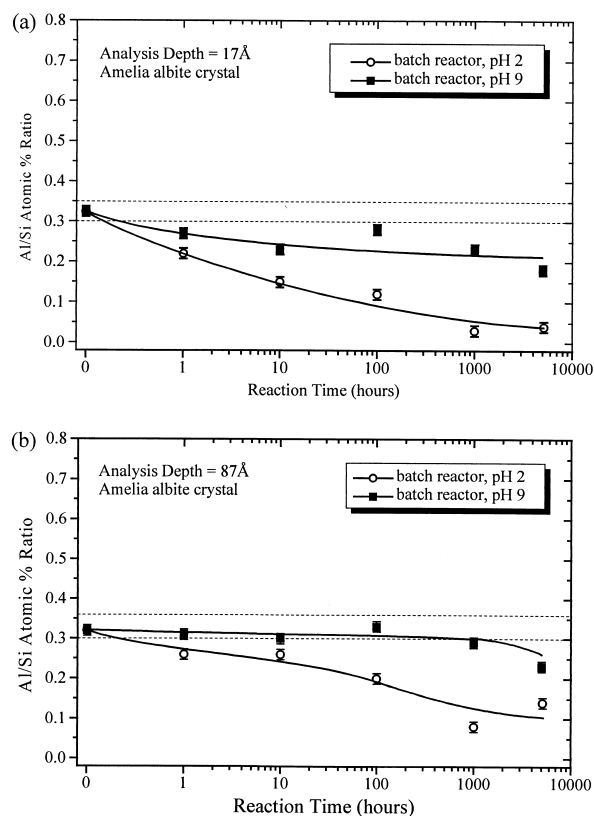


Fig. 7. Al/Si ratios (atomic %) as measured with (a) ARXPS (analysis depth = 17 Å) and (b) XPS (analysis depth = 87 Å), plotted as a function of reaction time for Amelia albite crystal plates in pH 2 and pH 9 solutions in batch reactors at 25°C. The dashed lines represent the highest and lowest Al/Si ratios measured on 10 unreacted, polished crystal surfaces. The curves are provided to guide the reader's eye.

the range 17–87 Å in almost all cases. The only exception was Na leaching in the glass at pH 2; but even in this case, the SIMS hydrogen depth profile (in Fig. 9) showed enrichment to a depth ≤ 500 Å.

FTIR absorbance spectra of the glass surfaces reacted in pH 2 solutions (Fig. 10) and pH 9 (not shown) were also identical to that of the unreacted glass surfaces, indicating no significant change in the structure of the glass surface. The peak at 1054 cm^{-1} was assigned to antisymmetric stretching vibrations of bridging Si-O-Si bonds within SiO_4 tetrahedra (Sanders et al., 1974; Doremus, 1980; Husung and Doremus, 1990; Roy, 1990) and the peak at 464 cm^{-1} was assigned to Si-O-Si and O-Si-O bending vibrations (sometimes referred to as Si-O-Si rocking vibration) (Husung and Doremus, 1990). The analysis depth of this technique is $> \sim 1\text{ }\mu\text{m}$ at 1250 – 900 cm^{-1} and further confirms the limited thickness of the altered surface layers.

4. DISCUSSION

4.1. Dissolution Rates

All dissolution rates are summarized in Table 5 as release rate of Si normalized by initial surface area. As per the observations of Casey et al. (1989), we saw no increase in dissolution rate with time for the glass dissolved at pH 2. We therefore

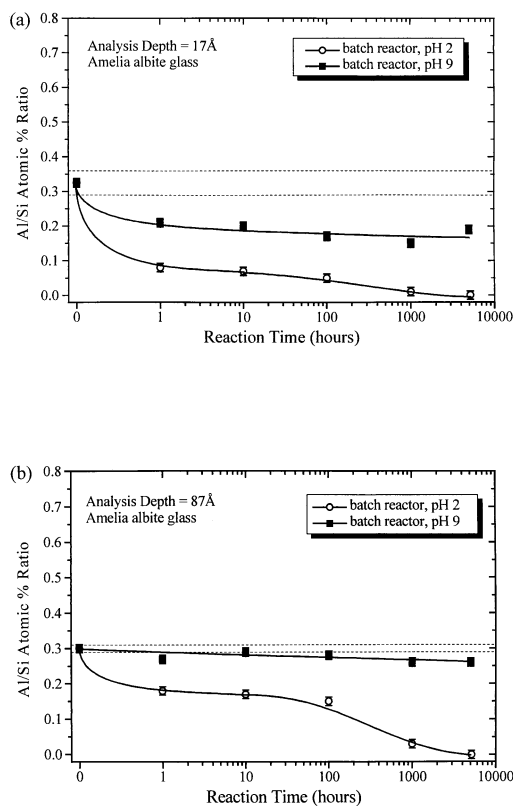


Fig. 8. Al/Si ratios (atomic %) as measured with (a) ARXPS (analysis depth = 17 Å) and (b) XPS (analysis depth = 87 Å), plotted as a function of reaction time for Amelia albite glass plates in pH 2 and pH 9 solutions in batch reactors at 25°C. The dashed lines represent the highest and lowest Al/Si ratios measured on 10 unreacted, polished glass surfaces. The curves are provided to guide the reader's eye.

interpret the increase in specific surface area of the glass dissolved at pH 2 as the result of the formation and spalling of a porous surface layer. This increase in specific surface area is not interpreted as an increase in reactive area; all rates are thus normalized by initial surface area. The steady state dissolution rates of crystalline albite are higher in acid (pH 2) than in

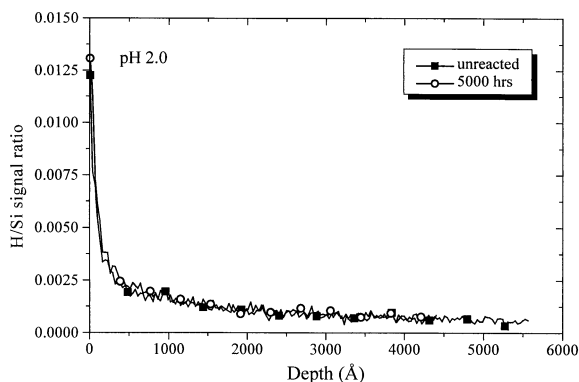


Fig. 9. SIMS hydrogen depth profiles of unreacted and reacted albite glass.

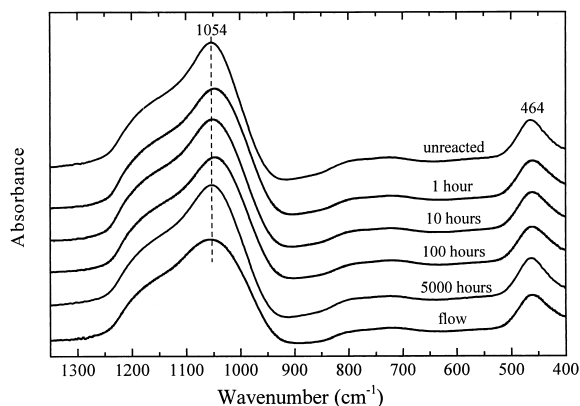


Fig. 10. FTIRRS absorbance spectra of unreacted and reacted albite glass at pH 2 in batch and flow reactors, 25°C.

neutral (pH 5.6) and weakly basic solutions (pH 8.4), and are in good agreement with data available in the literature (see Blum and Stillings, 1995 for a review). Moreover, the steady state dissolution rate of albite crystal is slightly higher at pH 8.4 than pH 5.6, which also agrees with data available for crystalline albite. The steady state dissolution rates of albite glass at 25°C are identical, within error ($\pm 40\%$), to that of albite crystal at each pH. These results agree well with the observations of Zellmer (1986) at 70°C, Shade (1981) at 90°C, and Hellmann et al. (1990b) at 300°C, except that Hellmann reported a large difference in the glass and crystal rates in the neutral-basic region (pH 5.7–11.0). Although rates at pH 5.6 and 8.4 for glass and crystal were identical within error in our experiments at 25°C, glass dissolution rates were slightly faster than crystal dissolution rates, in agreement with the observations of Hellmann.

4.2. Altered Layers

Solution analysis indicates that steady state is achieved much more rapidly at pH 2 (~1000 hours) than at pH 5.6 (3500 h) and pH 8.4 (3000 h). Faster approach to steady state correlates with faster dissolution in acidic conditions as compared to neutral or basic pH. Solution analysis also indicates that all of the solutions are undersaturated with respect to gibbsite at the end of each experiment. At pH 2, 5.6, and 8.4 the solubilities of gibbsite are $>1 \times 10^7$ ppm, 20 ppb, and 30 ppb Al, respectively (based on data from Stumm and Morgan, 1996). At the end of the experiments with crystal at pH 2, 5.6, and 8.4, the Al concentrations were 152 ppb, 7 ppb, and 8 ppb, respectively, and with glass were 166 ppb, 7 ppb, and 9 ppb, respectively. Thus, solutions at pH 5.6 and 8.4 are closer to saturation with respect to gibbsite than at pH 2.

While it has been shown that steady state (constant Si concentration ($\pm 10\%$)) was achieved by the end of each experiment, solution analysis indicates that the release of Na and Si was not always stoichiometric (Table 5). The degree of stoichiometry is summarized in Table 5 as the ratio of the Na and Al release rates with respect to the Si release rate. If the Na/Si and Al/Si ratios are equal to 0.33, then the release of Na, Al, and Si is stoichiometric. If one of these ratios is >0.33 , Na or

Al is released faster than Si and if these ratios are <0.33 , Na or Al is being released slower than Si. At steady state, the release of Al was stoichiometric within error for both the glass and crystal at each pH, and was stoichiometric within error for crystal dissolved at low and high pH. However, the release of Na was always faster than the release of Si for glass over the entire pH range and for crystal at neutral pH. Furthermore, the glass was always further from stoichiometry than the crystal. This data indicates that at steady state, a constant leached layer thickness was achieved with respect to Al leaching on glass and crystal at all pHs, but the layer was still growing with respect to Na leaching for the glass surfaces. At neutral pH, Na leaching may have been continuing for both glass and crystal.

Despite similarity in the steady state dissolution rates of crystalline and amorphous albite, Na and Al depletion is more extensive from the glass surface than the crystal surface, especially at pH 2. However, within the outer 17 Å, the outermost surfaces of the glass and crystal are compositionally similar (Table 4). These observations may be related to structural differences between crystal and glass as described below.

Structures of altered layers on crystalline albite are presumed to be more open and porous than the unaltered crystal surface (Casey and Bunker, 1990; Hellmann, 1995; Hellmann, 1997b), allowing proton-bearing species access deep within the surface. In this respect, the altered surface layer of albite may be similar to the glass. Albite glass ($\sim 2.38 \text{ g/cm}^3$) consists predominantly of 6-membered rings of tetrahedra while crystalline albite ($\sim 2.62 \text{ g/cm}^3$) consists predominantly of 4-membered rings (Taylor and Brown, 1979). Interdiffusion of proton-bearing or other aqueous species (such as H_3O^+ , H_2O , H^+ , Li^+ , OH^- , Cl^-) and modifier ions should be easier in the more open glass structure, explaining the higher depletion of Na and Al from the glass surface than from the crystal surface. Apparently, however, any enhancement of dissolution rate due to more extensive depletion from the glass surface is small ($<$ a factor of 3) at all values of pH. The similarity of chemistry of the outer surface layer (depth of tens of Ångströms) and the similarity in rate observed for the glass and crystal suggests that the outer layer controls the dissolution rate.

The large change in the specific surface area of the glass at pH 2 is consistent with development of an extensive, highly porous altered layer. The smaller increase in specific surface area of the crystal is consistent with the formation of a less extensive, but still highly porous and open altered layer. Despite this difference in final surface area, the glass and crystal dissolve at the same rate at pH 2 when normalized to initial surface areas. This information, combined with the ARXPS data, corroborates the finding that structure and chemistry of the outermost crystal and glass surfaces ($<17 \text{ Å}$) are similar and control the dissolution rate.

Similarity in the dissolution rates of crystalline and amorphous albite at low pH is consistent with models in which reactions at the surface and within a thin ($<20 \text{ Å}$) altered surface control the dissolution rate. Any effect of the deeper portions of the altered layer on the dissolution rate is unmeasurable in this type of experiment.

In contrast to extensive leaching at pH 2, XPS at a high angle ($\theta = 65^\circ$, $D = 87 \text{ Å}$) indicates less depletion of Na and Al from surfaces dissolved in solutions at pH 5.6 and 8.4 and little or no surface layer formation. However, ARXPS at a lower angle

($\theta = 10^\circ$, $D = 17 \text{ Å}$) documents some depletion of Na and/or Al, indicating the formation of thin altered surface layers in neutral and weakly basic conditions. In contrast to observations based on solution chemistry by Chou and Wollast (1984), who reported Al enrichment and Si depletion in neutral and basic conditions at 25°C , these results show that enrichment of the glass or crystal surface in aluminum does not occur in neutral or weakly basic solutions. These results agree substantially with observations at higher temperature (Hellmann et al., 1995). Again, we hypothesize that the chemistry of these outer layers controls dissolution rate.

4.3. Natural Glasses

Geochemists may be surprised that the dissolution rate of albite glass is similar to that of crystalline albite (within a factor of 3) since glasses from volcanic rocks older than the Miocene (~ 15 million years) do not generally exist (see White and Claassen, 1980; White, 1984). Dissolution of tektite glasses, however, is very slow; these glasses have existed in nature for up to 35 million years (Glass, 1984). This difference in dissolution rate between volcanic and tektite glasses may be related to the water content of the glasses. Rhyolitic glasses contain ~ 4 wt% water while tektite glasses contain <1 wt% water (O'Keefe, 1964; Gilchrist et al., 1969). Chemical durability of $\text{Na}_2\text{O}-3 \text{ SiO}_2$ glasses decreases rapidly as the water content increases over a range of 0–5 wt% (Tomazawa et al., 1982).

If the water content in our albite glass equals the difference between 100% and the sum of the oxide constituents (e.g., Yang and Kirkpatrick, 1989), then the water content was ~ 1.1 wt% (Table 3). Such a water content should not appreciably enhance dissolution of the glass matrix, if this albitic glass reacts similarly to the glasses studied by Tomazawa et al. (1982). Therefore, where water content of natural glasses is higher than the glass used here, dissolution rates may also be correspondingly higher. Higher water contents in natural glasses may therefore explain why glasses disappear more readily than crystalline material in natural systems.

Glasses may also dissolve more rapidly than crystals in nature if weathering solutions are close to equilibrium with the crystals. Thus, a small difference in dissolution rate measured in our experiments may translate into larger differences in dissolution rate between glass and crystal under natural conditions. Furthermore, small differences in dissolution rate in the laboratory can translate into large differences in extent of dissolution when extrapolated to geologic time frames.

Another explanation for the enhanced reactivity of natural glasses may lie in the fact that most natural glasses are generally not pure feldspar in composition, and other glass compositions may be more reactive than their crystalline counterparts. In this study, the crystals were carefully chosen so that the composition of glass and crystal would be nearly identical, and the effects of crystallinity alone could be evaluated. More tests will be needed, however, to determine whether similarity in dissolution rate between glass and mineral of identical composition is a general observation.

5. CONCLUSIONS

Crystalline and amorphous albite release Si and Al at comparable rates ($\pm 40\%$) as measured in acid (pH 2), water (pH

5.6) and base (pH 8.4) at 25°C. In acid, Na and Al depletion is more extensive from the glass surface than the crystal surface although ARXPS indicates severe depletion of Na and Al from both the crystal and glass surfaces within the outermost 17 Å at pH 2. The more extensive in-depth alteration for the glass is probably due to the less dense, 6-membered ring structure of the bulk glass compared to the 4-membered ring structure of the crystal. Similarities in steady state surface composition ($< \sim 20$ Å) and dissolution rates suggest that the 'altered' crystal surface and 'altered' glass surface adjacent to the liquid phase are key to the control of dissolution rate (i.e., the solid/liquid interface affects rates more than the in-depth leached layers). BET suggests that the structure of the surface layers on BOTH the crystal and glass are more open than their bulk structures, and presumably controls the attack and transport of proton-bearing species at both the glass and crystal surface. In neutral and weakly basic conditions, XPS indicates the formation of less extensive altered surface layers on both albite glass and crystal than in acidic conditions. The compositions of these surfaces are depleted in Na and/or Al, but do not exhibit enrichment of Al (contrary to previous reports in the literature). In neutral and weakly basic solutions, the dissolution rates of albite glass and crystal are similar but lower than in acid conditions. Overall, the results of this study indicate that the thickness of the leached layer does not measurably affect the dissolution rates of the feldspar crystal and glass as measured in flow experiments at 25°C (rates measured to within $\pm 40\%$). The similarity in rate of dissolution between crystal and glass of albite composition may also indicate that future geochemical studies of mineral dissolution could be more efficiently completed in some cases by investigation of glass, which can be made homogeneous, rather than crystalline material, which is typically variable in impurity and defect content and whose microstructure compromises surface analysis.

Acknowledgments—The authors would like to thank Henry Gong, Shaole Wu, Mark Angelone, and Vince Bojan of the Materials Characterization Laboratory and Don Voigt and Will White of the Department of Geosciences at Penn State University for their assistance with sample characterization and experimental design. This research was supported by the Department of Energy (DE-FG02-95ER14547.A000). We also thank Roland Hellmann and one anonymous reviewer for excellent reviews. Alex Blum and Art White of the U.S. Geological Survey are acknowledged for discussions of natural glass dissolution.

REFERENCES

- Berner R. A. and Holdren G. R., Jr. (1979) Mechanism of feldspar weathering-II. Observations of feldspars from soils. *Geochim. Cosmochim. Acta* **43**, 1173–1186.
- Blum A. and Lasaga A. (1988) Role of surface speciation in the low-temperature dissolution of minerals. *Nature* **331**, 431–433.
- Blum A. E. and Lasaga A. C. (1991) The role of surface speciation in the dissolution of albite. *Geochim. Cosmochim. Acta* **55**, 2193–2201.
- Blum A. E. and Stillings L. L. (1995) Feldspar dissolution kinetics. In *Chemical Weathering Rates of Silicate Minerals* (eds. A. F. White and S. L. Brantley); *Reviews in Mineralogy*, Vol. 31, pp. 291–351. Mineral. Soc. Amer.
- Brady P. V. and Walther J. V. (1989) Controls on silicate dissolution rates in neutral and basic pH solutions at 25°C. *Geochim. Cosmochim. Acta* **53**, 2823–2830.
- Brady P. V. and Walther J. V. (1992) Surface chemistry and silicate dissolution at elevated temperatures. *Am. J. Sci.* **292**, 639–658.
- Brantley S. L. and Stillings L. (1996) Feldspar dissolution at 25°C and low pH. *Am. J. Sci.* **296**, 101–127.
- Brantley S. L. and Stillings L. (1997) Reply: Feldspar dissolution at 25°C and low pH. *Am. J. Sci.* **297**, 1021–1032.
- Casey W. H., Westrich H. R., Massis T., Banfield J. F., and Arnold G. W. (1989) The surface of labradorite feldspar after acid hydrolysis. *Chem. Geol.* **78**, 205–218.
- Casey W. H. and Bunker B. (1990) Leaching of mineral and glass surfaces during dissolution. In *Mineral-Water Interface Geochemistry* (eds. M. F. Hochella, Jr. and A. F. White); *Reviews in Mineralogy*, Vol. 23, pp. 397–425. Mineral. Soc. Amer.
- Chen Y. and Brantley S. L. (1997) Temperature- and pH-dependence of albite dissolution rate at acid pH. *Chem. Geol.* **135**, 275–290.
- Chen Y., Brantley S. L., and Ilton E. S. (2000) X-ray photoelectron spectroscopic measurement of the temperature dependence of cations from the albite surface. *Chem. Geol.* **163**, 115–128.
- Chou L. and Wollast R. (1984) Study of the weathering of albite at room temperature and pressure with a fluidized bed reactor. *Geochim. Cosmochim. Acta* **48**, 2205–2217.
- Doremus R. H. (1975) Interdiffusion of hydrogen and alkali ions in a glass surface. *J. Non-Cryst. Solids* **19**, 137–144.
- Doremus R. H. (1980) Infrared spectroscopy of surfaces of glasses containing alkali ions. *J. Non-Cryst. Solids* **41**, 145–149.
- Doremus R. H. (1994) Chemical durability: Reaction of water with glass. In *Glass Science (2nd Ed.)*, pp. 215–240. John Wiley & Sons Inc.
- Douglas R. W. and El-Shamy T. M. M. (1967) Reactions of glasses with aqueous solutions. *J. Am. Ceram. Soc.* **50**, 1–8.
- Furrer G. and Stumm W. (1986) The coordination chemistry of weathering. I. Dissolution kinetics of δ -Al₂O₃ and BeO. *Geochim. Cosmochim. Acta* **50**, 1847–1860.
- Gautier J.-M., Oelkers E. H., and Schott J. (1994) Experimental study of K-feldspar dissolution rates as a function of chemical affinity at 150°C and pH 9. *Geochim. Cosmochim. Acta* **58**, 4549–4560.
- Gilchrist J., Thorpe A. N., and Senftle F. E. (1969) Infrared analysis of water in tektites and other glasses. *J. Geophys. Res.* **74**, 1475–1483.
- Glass B. P. (1984) Tektites. *J. Non-Cryst. Solids* **67**, 333–344.
- Gout R., Oelkers E. H., Schott J., and Zwick A. (1997) The surface chemistry and structure of acid-leached albite: New insights on the dissolution mechanism of alkali feldspar. *Geochim. Cosmochim. Acta* **61**, 3013–3018.
- Grambow B. (1992) Geochemical approach to glass dissolution. In *Corrosion of Glass, Ceramics and Ceramic Superconductors* (eds. D. E. Clark and B. K. Zaitos), pp. 124–152. Noyes Publications.
- Hellmann R., Eggleston C. M., Hochella M. F., Jr., and Crerar D. A. (1989) Altered layers on dissolving albite-I. Results In *Water-Rock Interaction WRI-6* (ed. D. L. Miles), pp. 293–296. A. A. Balkema.
- Hellmann R., Eggleston C. M., Hochella M. F., Jr., and Crerar D. A. (1990a) The formation of leached layers on albite surfaces during dissolution under hydrothermal conditions. *Geochim. Cosmochim. Acta* **54**, 1267–1281.
- Hellmann R., Schott J., Dran J.-C., Petit J.-C., and Della Mea G. (1990b) A comparison of the dissolution behavior of albite and albite glass under hydrothermal conditions. *Geol. Soc. Amer. Ann. Mtg. Abstr.*, (abstr.) p. A292.
- Hellmann R., Schott J., Dran J.-C., Petit J.-C., and Della Mea G. (1991) The formation of leached layers on hydrothermally altered albite and albite glass. *EUG 6 (Abstr.)* **3**, p. 468.
- Hellmann R. (1994) The albite-water system: Part I. The kinetics of dissolution as a function of pH at 100, 200, and 300°C. *Geochim. Cosmochim. Acta* **58**, 595–611.
- Hellmann R. (1995) The albite-water system: Part II. The time-evolution of the stoichiometry of dissolution as a function of pH at 100, 200, and 300°C. *Geochim. Cosmochim. Acta* **59**, 1669–1697.
- Hellmann R., Dran J.-C., and Della Mea G. (1997a) The albite-water system: Part III. Characterization of leached and hydrogen-enriched layers formed at 300°C using MeV ion beam techniques. *Geochim. Cosmochim. Acta* **61**, 1575–1594.
- Hellmann R. (1997b) The albite-water system: Part IV. Diffusion modeling of leached and hydrogen-enriched layers. *Geochim. Cosmochim. Acta* **61**, 1595–1611.
- Hellmann R. (1997c) Hydrogen penetration of minerals and glasses during hydrolysis at hydrothermal conditions. *7th Annual Goldschmidt Conference (Abstr.)* p. 91.

- Holdren G. R., Jr. and Berner R. A. (1979) Mechanism of feldspar weathering-I. Experimental studies. *Geochim. Cosmochim. Acta* **43**, 1161–1171.
- Husung R. D. and Doremus R. H. (1990) The infrared transmission spectra of four silicate glasses before and after exposure to water. *J. Mater. Res.* **5**, 2209–2217.
- Kubicki J. D. and Sykes D. (1993) Molecular orbital calculations of vibrations in three-membered aluminosilicate rings. *Phys. Chem. Mineral.* **19**, 381–391.
- Merzbacher C. I. (1987) The structure of alkaline earth aluminosilicate glasses and melts: A spectroscopic study. Ph.D. thesis, The Pennsylvania State University.
- Merzbacher C. I. and White W. B. (1988) Structure of Na in aluminosilicate glasses: A far-infrared reflectance spectroscopic study. *Am. Mineral.* **73**, 1089–1094.
- Muir I. J., Bancroft G. M., Shotyk W., and Nesbitt H. W. (1990) A SIMS and XPS study of dissolving plagioclase. *Geochim. Cosmochim. Acta* **54**, 2247–2256.
- O'Keefe J. A. (1964) Water in tektite glass. *J. Geophys. Res.* **69**, 3701–3707.
- Oelkers E. H., Schott J., and Devidal J.-L. (1994) The effect of aluminum, pH, and chemical affinity on the rates of aluminosilicate dissolution reactions. *Geochim. Cosmochim. Acta* **58**, 2011–2024.
- Oelkers E. H. and Schott J. (1995a) Experimental study of anorthite dissolution and the relative mechanism of feldspar hydrolysis. *Geochim. Cosmochim. Acta* **59**, 5039–2053.
- Oelkers E. H. and Schott J. (1995b) The dependence of silicate dissolution rates on their structure and composition. In *Water-Rock Interaction WRI-8* (eds. Y. K. Kharaka and O. V. Chudaev), pp. 153–156. A. A. Balkema.
- Petrovic R., Berner R., and Sjoberg E. L. (1976) Rate control in dissolution of alkali feldspars-I. Study of residual feldspar grains by X-ray photoelectron spectroscopy. *Geochim. Cosmochim. Acta* **40**, 537–548.
- Robie R. A., Hemingway B. S., and Fisher G. R. (1978). Thermodynamic properties of minerals and related substances at 298.15 K and 1 bar pressure and at higher temperatures. *U.S. Geological Survey Bulletin* 1452, 456.
- Roy B. N. (1990) Infrared spectroscopy of lead and alkaline-earth aluminosilicate glasses. *J. Am. Ceram. Soc.* **73**, 846–855.
- Sanders D. M., Person W. B., and Hench L. L. (1974) Quantitative analysis of glass structure with the use of infrared reflectance spectra. *Appl. Spectrosc.* **28**, 247–255.
- Schott J. (1990) Modeling of the dissolution of strained and unstrained multiple oxides: The surface speciation approach. In *Aquatic Chemical Kinetics* (ed. W. Stumm), pp. 293–315. Wiley Interscience.
- Seah M. P. and Dench W. A. (1979) Quantitative electron spectroscopy of surfaces: A standard data base for electron inelastic mean free paths in solids. *Surface Interface Anal.* **1**, 2–11.
- Shade J. W. (1981) Comparison of glass and ceramic leaching behavior by natural analogs. *Nucl. Chem. Waste Manage.* **2**, 219–228.
- Smets B. M. J. and Lommen T. P. A. (1982) The leaching of sodium aluminosilicate glasses studied by secondary ion mass spectrometry. *Phys. Chem. Glasses* **23**, 83–87.
- Stillings L. L. (1994) The surface chemistry and dissolution kinetics of feldspar. Ph.D. Dissertation, Department of Geosciences, The Pennsylvania State University, University Park, Pa.
- Stillings L. L. and Brantley S. L. (1995) Feldspar dissolution at 25°C and pH 3: Reaction stoichiometry and the effect of ionic strength. *Geochim. Cosmochim. Acta* **59**, 1483–1496.
- Stumm W. and Morgan J. J. (1996) *Aquatic Chemistry; Chemical Equilibria and Rates in Natural Waters*. 3rd Ed. John Wiley and Sons, Inc.
- Sykes D. and Kubicki J. D. (1996) Four-membered rings in silica and aluminosilicate glasses. *Am. Mineral.* **81**, 265–272.
- Taylor M. and Brown G. E., Jr. (1979) Structure of mineral glasses-I. The feldspar glasses NaAlSi₃O₈, KAlSi₃O₈, CaAl₂Si₂O₈. *Geochim. Cosmochim. Acta* **43**, 61–75.
- Tomazawa M., Erwin C. Y., Takata M., and Watson E. B. (1982) Effect of water content on the chemical durability of Na₂O-3SiO₂ glass. *J. Am. Ceram. Soc.* **65**, 182–183.
- Tsuzuki Y., Kadota S., and Takashima I. (1985) Dissolution process of albite and albite glass in acid solutions at 47°C. *Chem. Geol.* **49**, 127–140.
- Vig J. R. (1992) Ultraviolet-ozone cleaning of semiconductor surfaces. *Research and Development Technical Report Number SLCT-TR-91-33 (Rev. 1)*. Army Research Laboratory, Electronics and Power Sources Directorate, Fort Monmouth, NJ.
- Walther J. V. (1997) Comment: Feldspar Dissolution at 25°C and low pH. *Am. J. Sci.* **297**, 1012–1021.
- White A. F. and Claassen H. C. (1980) Kinetic model for the short-term dissolution of a rhyolitic glass. *Chem. Geol.* **28**, 91–109.
- White A. F. (1984) Weathering characteristics of natural glass and influences on associated water chemistry. *J. Non-Cryst. Solids* **67**, 225–244.
- White W. B. (1992) Theory of corrosion of glass and ceramics. In *Corrosion of Glass, Ceramics and Ceramic Superconductors* (eds. D. E. Clark and B. K. Zaitos), pp. 2–28. Noyes Publications.
- Yang W.-H. A. and Kirkpatrick R. (1989) Hydrothermal reaction of albite and a sodium aluminosilicate glass: A solid-state NMR study. *Geochim. Cosmochim. Acta* **53**, 805–819.
- Zellmer L. A. and White W. B. (1986) The comparative dissolution kinetics of albite crystals and albite glass in aqueous solutions at 70°C. In *Fifth International Symposium on Water-Rock Interactions, Extended Abstracts* **5**, 652–655.
- Zellmer L. A. (1986) Dissolution kinetics of crystalline and amorphous albite. M. Sc. thesis, The Pennsylvania State University, University Park, Pa.